



14th IEA Heat Pump Conference
15-18 May 2023, Chicago, Illinois

Analysis of the performance of a heat pump with subcooling control as a function of the refrigerant charge

Belén Llopis-Mengual^a, Emilio Navarro-Peris^{a*}

^aInstituto Universitario de Investigación de Ingeniería Energética (IUIIE), Universitat Politècnica de València (UPV), Camino de Vera s/n, 46022, Valencia, Spain

Abstract

When using hydrocarbons like propane (R290) as a refrigerant in heat pumps, it is critical to detect if the system is undercharged to find potential leaks, as they are flammable. This is specially challenging in reversible air-to-water heat pumps where a liquid receiver to compensate for the charge fluctuations is commonly installed. This liquid receiver introduces some tolerance of the system to charge fluctuations which are desirable from the system performance point of view but also makes especially difficult the pre-diagnosis of a possible leak. This study has experimentally characterized the performance with different refrigerant charge levels of a reversible air-to-water propane heat pump with a liquid receiver at the compressor inlet and a variable-speed compressor. It has different control strategies: superheat control for cooling and subcooling for heating mode. The work shows the evolution of the most important system variables like discharge, condensation, and evaporation temperature, as well as subcooling and superheat, and which could be the impact on the system performance. Finally, the use of compressor speed as a tool to diagnose potential system undercharge faults have been pointed out as a promising strategy.

© HPC2023.

Selection and/or peer-review under the responsibility of the organizers of the 14th IEA Heat Pump Conference 2023.

Keywords: refrigerant charge; subcooling control; air-to-water heat pump; undercharge fault; R290

1. Introduction

Nowadays, attempts are being made to reduce the energy consumption in heating, cooling, and domestic hot water, since it accounts for the 80% of the energy that citizens consume [1]. Heat pumps that use outdoor air to heat water for heating and domestic hot water can undoubtedly contribute to this. In addition, if they are reversible, they can also provide cold water for air-conditioning. According to [2], heat pump sales grew by 34% in Europe in 2022, and within a short period of time, heat pump installations are expected to increase.

Concerning the refrigerants used in these systems, the European Union currently restricts a large number of hydrofluorocarbons (HFCs), which are the ones that have been used the most. The main alternatives, harmless to the ozone layer and without influence upon the greenhouse effect, are natural refrigerants such as carbon dioxide, ammonia, and hydrocarbons. However, the latter has a safety problem, given the refrigerant's flammability. Thus, it is critical to detect if refrigerant charge leakage occurs. Sensors that detect this are currently expensive or require much maintenance and must be replaced regularly. Besides, understanding how the system will behave if this fault occurs is also essential for early detection and proper maintenance.

Many experimental tests have been conducted to evaluate the system performance with refrigerant charge variation. For example, [3] analyzes the performance with the charge level of several split and rooftop air-source heat pumps with refrigerants R410A and R407C and with different compressors and expansion devices. Another is [4], which also imposes different refrigerant charge levels, among other faults, to a split residential heat pump in cooling mode with a Thermal Expansion Valve, measuring the effect on variables with these faults. In this work [5], they use experimental tests with different refrigerant charge levels to generate a virtual

* Corresponding author. Tel.: +34963879123
E-mail address: emilio.navarro@iie.upv.es

refrigerant charge sensor. They use several types of systems, both air-to-air and water-to-water, with variable speed compressors and some of them reversible for cooling and heating, with accumulators at the condenser outlet to compensate for different charge requirements between modes. In the latter case, they conclude that their virtual sensor does not work well with higher refrigerant levels in the accumulator because charge variations did not significantly change the vapor compression cycle variables. A similar conclusion is reached in this study [6], in which they simulate undercharge faults in a refrigeration system with a liquid line receiver but obtain significant differences in the prediction of system variables under low charge conditions due to the presence of the accumulator.

Nevertheless, there are few studies on reversible air-to-water heat pumps on their performance depending on the refrigerant charge. In this type of system, the analysis is essential because when changing between cooling or heating modes, the refrigerant charge requirements and the difference in internal volume between heat exchangers generate particular behaviors. In this study [7], they experimentally analyze the refrigerant mass distribution of each component of the cycle in an invertible air-to-water heat pump with R32, showing significant differences in the refrigerant charge distribution depending on the conditions.

To address this issue, some studies like [8] have shown that it is beneficial for such reversible systems to use an accumulator in the compressor suction to compensate for charge variations depending on the mode of operation. With this, the subcooling is regulated by the expansion valve instead of the superheat. Besides, some works as [9] study different subcooling control strategies with this system to optimize the performance of a heat pump.

In the present work, it is experimentally investigated the influence of the charge in a reversible air-to-water propane heat pump with different operating modes: cooling mode with superheat control and heating mode with subcooling control. The system has an accumulator at the compressor suction and uses a variable-speed compressor. The study analyzes the variables that would allow the detection of refrigerant leaks in this system in heating mode, given its particularity of subcooling control with an accumulator in the compressor suction which acts as a charge reservoir.

2. Methodology

2.1. Experimental setup

In this study, it is conducted an experimental campaign with a reversible air-to-water heat pump with 7 kW of nominal capacity that uses R290 (propane) as a refrigerant. Figure 1 shows the schematic of the system, whose main components are: a rotary variable speed compressor, a brazed plate heat exchanger (BPHX), a finned-tube heat exchanger, an electronic expansion valve (EEV), and a liquid accumulator at the compressor suction. In addition, the system has a reversible valve or 4-way valve for switching between modes.

The main differences between modes are the following. In cooling mode, the BPHX is the evaporator used to cool water, and the EEV maintains a constant superheat (SH) at the compressor suction (the superheat is taken as the difference between the compressor inlet temperature and the evaporation temperature). However, in heating mode, the BPHX is used as a condenser to heat water, and the EEV maintains a constant subcooling (SC) at the condenser outlet (the subcooling is taken as the difference between the condensing temperature and the condenser outlet temperature). The manufacturer designs this heat pump with the target of optimizing the heating mode. This mode is the one in which the system is going to work more hours during the year.

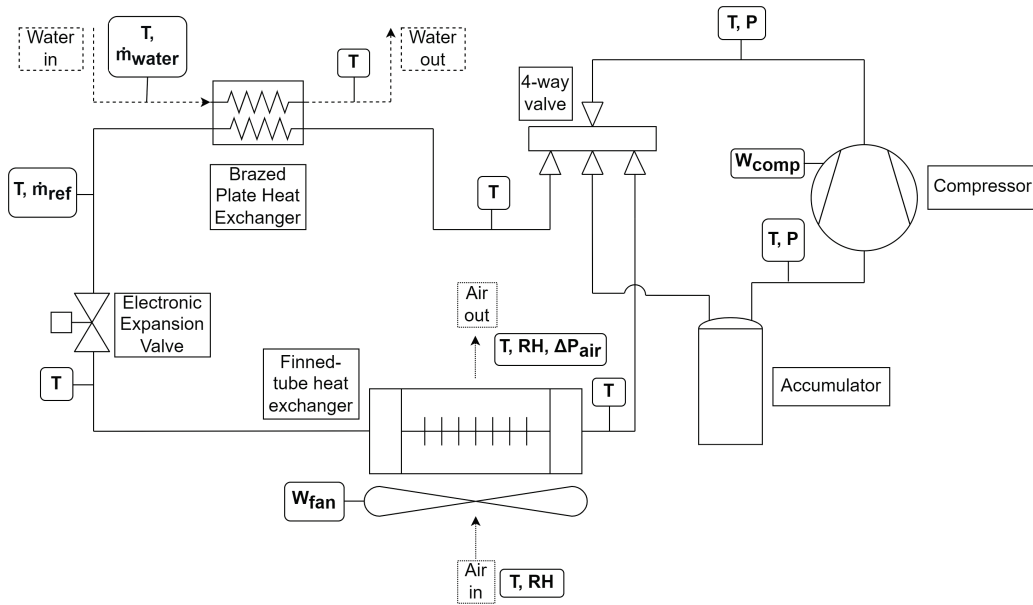


Fig. 1. Experimental setup of the reversible air-to-water heat pump

The unit is tested in a psychrometric chamber capable of recreating the needed working conditions of the heat pump. Figure 1 shows the location of the sensors in the system. These are compressor suction and discharge pressure, refrigerant temperature before and after each component, and water and air temperature. In addition, the refrigerant mass flow rate in heating mode was measured with a Coriolis flowmeter installed at the outlet of the BPHX (condenser in heating). To obtain the refrigerant flow rate in cooling mode, it was measured the water flow rate with a Coriolis flowmeter. From this, it is obtained the refrigerant flow rate with the corresponding balance in the BPHX. In addition, an averaging pitot tube flowmeter is used to obtain the fan’s airflow. The refrigerant charge used in each test is measured with a Gram LHK-150 scale, with a resolution of 10g. Table 1 lists the instruments used and their range and total error from the uncertainty analysis.

Table 1. Measurement instruments and their range and uncertainties.

Measurement	Instrument	Range	Total error
Refrigerant temperature	Thermocouple type T	-270-400 °C	±0.8 (°C)
Water and air temperature	Thermoresistance PT-100	-220-850 °C	±0.07 (°C)
Suction and discharge pressure	Pressure transducer Rosemount 3051	0-15 bar (suction) 10-45 bar (discharge)	±0.06 (bar)
Refrigerant mass flow rate	Coriolis flowmeter Micro Motion CMFS015M	0-5600 kg/h	±0.13 (kg/h)
Water mass flow rate	Coriolis flowmeter Mass 2100	0-245 kg/h	±4.48 (kg/h)
Air relative humidity	Vaisala Humicap 180	0-100%	±2.77 (%)
Pressure drop in the air heat exchanger	Differential pressure transducer DPT-4001	0-25 Pa	±0.2 (Pa)

2.2. Test campaign

Table 2 shows the conditions at which the unit is tested. These correspond to both modes of operation, different air and water inlet conditions, and compressor speeds. Each of these conditions is tested for a range of refrigerant charges, which are defined as:

$$m_{ref}(\%) = \frac{m_{ref-test} - m_{ref-nominal}}{m_{ref-nominal}} \cdot 100 \quad (1)$$

Where $m_{ref-test}$ is the refrigerant charge at a given test and $m_{ref-nominal}$ the unit's nominal (standard) charge, indicated by the manufacturer. Thus, a refrigerant charge percentage of 85% means that the unit is charged with a 15% less refrigerant charge than the nominal that should have.

Table 2. Experimental testing conditions.

Mode	Test Condition	Inlet air dry bulb temperature (°C)	Inlet water temperature (°C)	Outlet water temperature (°C)	Compressor velocity (rps)	Refrigerant charge (%)
Cooling	A23W18-80rps	23	23	18	80	85, 90, 95, 100, 105, 110
	A35W7-30rps	35	12	7	30	
	A35W18-60rps	35	23	18	60	
Heating	A10W45-80rps	10	38	45	80	
	A12W24-40rps	12	20	24	40	
	A2W35-35rps	2	32	35	35	
	A7W70-80rps	7	64	70	80	

2.3. Heat pump model

In this study, a model of the air-source heat pump using the dedicated software IMST-ART has been built, see [10] for a detailed description. This software allows modeling and simulating vapor compression cycles with their real components in detail. Particularly, it is able to perform a detailed simulation of the heat exchangers based on the most relevant heat transfer, void fraction, and pressure drop correlations of the literature considering variables like refrigerant charge or oil in the system.

In order to build the model, detailed geometrical information about heat exchangers and the variable speed compressor must be supplied. In addition, the catalogue data's cooling capacity and compressor power input are introduced for different compressor speeds. When a compressor speed is set as an input, the model calculates interpolating between the various compressor speeds entered. Then, this is converted into volumetric and compressor efficiencies to calculate the whole cycle.

3. Results and discussion

3.1. Cooling mode

In cooling mode, the heat pump has 2 control strategies:

- Control a target SH to be maintained.
- Control a subcooling of 3 K. This second condition is activated when the water inlet temperature is 7°C or lower in order to avoid having evaporating temperatures lower than 0°C.

To analyze the results obtained after the experimental campaign, the inputs measured in each case have been introduced in the model with the nominal charge. Thus, the refrigerant charge needed by the system in those conditions has been calculated. Table 3 shows the inputs used and the necessary refrigerant charge calculated for each of them. Thus, A23W18-80rps and A35W18-60rps need a higher charge (0.34 and 0.35 kg, respectively) and A35W7-30rps a lower one (0.28 kg). In addition, the target SH of the system in the cases with higher charge is 5-6 K, while the one with the lower charge is around 0 K. This can be achieved by having a liquid accumulator at the outlet of the evaporator that allows having saturation conditions at its outlet.

Table 3. Refrigerant charge needed for each test condition in cooling mode.

Test condition	Air inlet temperature (°C)	Airflow (m3/h)	Water inlet temperature (°C)	Water outlet temperature (°C)	Compressor Speed (rps)	SC (K)	SH (K)	Total refrigerant charge (kg)
A23W18-80rps	23	732	23	18	80	18	5	0.34
A35W7-30rps	35	1257	12	7	30	3.5	0	0.28
A35W18-60rps	35	1226	23	18	60	14	6	0.35

Figure 2 shows the refrigerant charge accumulation in the A23W18-80rps condition, which needs 0.34 kg. Since in this condition, the target SH to be controlled is 5K, the accumulator at the outlet of the evaporator will be almost empty, and the refrigerant in the liquid state will be concentrated at the outlet of the condenser, which in cooling mode is the finned-tube. The SC measured with these conditions is 18K, a significant value since the refrigerant is located there. If the system is undercharged or refrigerant leakage occurs, the charge will be reduced from the condenser outlet, and therefore the main effect of observing is the SC, which decreases (Figure 4a). For the same reason, the condensation temperature (Figure 4b) will also be reduced. Figure 4c shows that the SH can be controlled even if the refrigerant charge increases or decreases to around 5K. Concerning the discharge temperature (Figure 4d), no significant changes are observed either since its variation with the charge will depend mainly on the state of the accumulator at the compressor's suction.

The A35W7-30rps condition requires less refrigerant charge than the previous one, and considering the low water temperature which introduces subcooling control instead of a superheat control, more charge will accumulate in the liquid state in the system (Figure 3). Thus, if refrigerant leakage occurs, it will reduce the amount of refrigerant in the accumulator, but SC (Figure 4a) or condensation temperature (Figure 4b) will be maintained at the same values. However, following Figure 4c, if the refrigerant charge is reduced to 90% of the nominal, it is observed that the measured SH, which controls the EEV, is 2K, and with 85% charge, 5K. It means that the refrigerant charge has been reduced from the accumulator. The system can no longer have saturation conditions at the outlet and maintain 0K of SH, changing the SH target. Furthermore, in Figure 4d, it is seen how the discharge temperature increases as the refrigerant charge is reduced since, by decreasing the level of liquid refrigerant in the accumulator, it enters with a higher vapor quality to the compressor, leading to a higher discharge temperature.

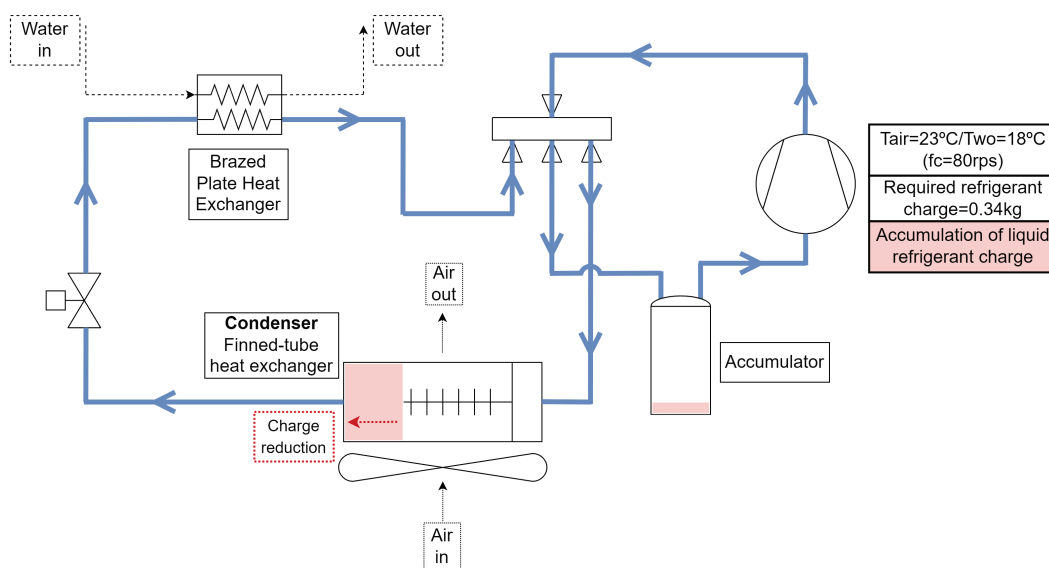


Fig. 2. Description of the accumulation of liquid refrigerant charge with the cooling mode condition of Tair=23°C/Two=18°C (fc=80rps).

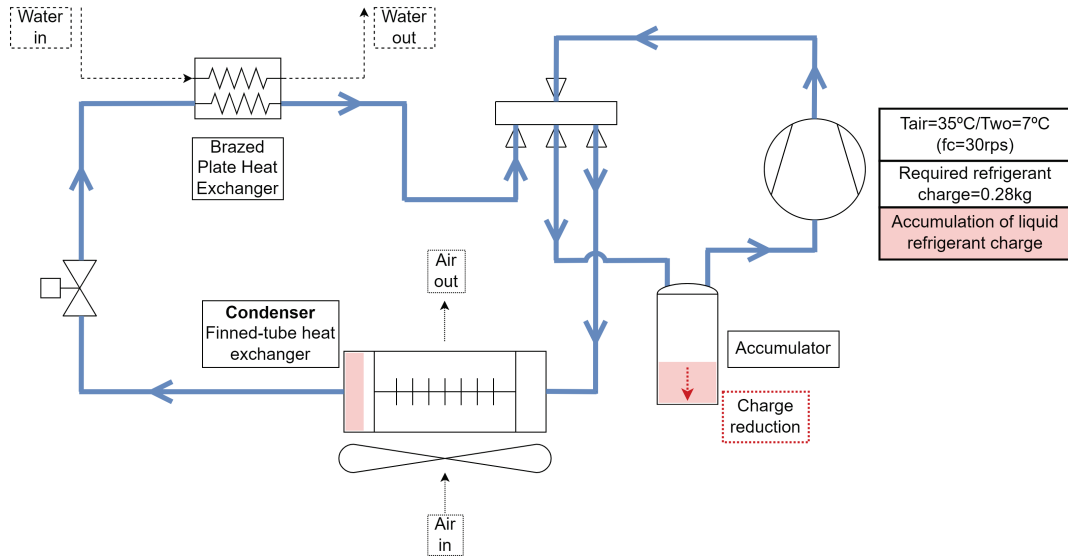


Fig. 3. Description of the accumulation of liquid refrigerant charge with the cooling mode condition of $T_{air}=35^{\circ}\text{C}/T_{wo}=7^{\circ}\text{C}$ ($fc=30\text{rps}$).

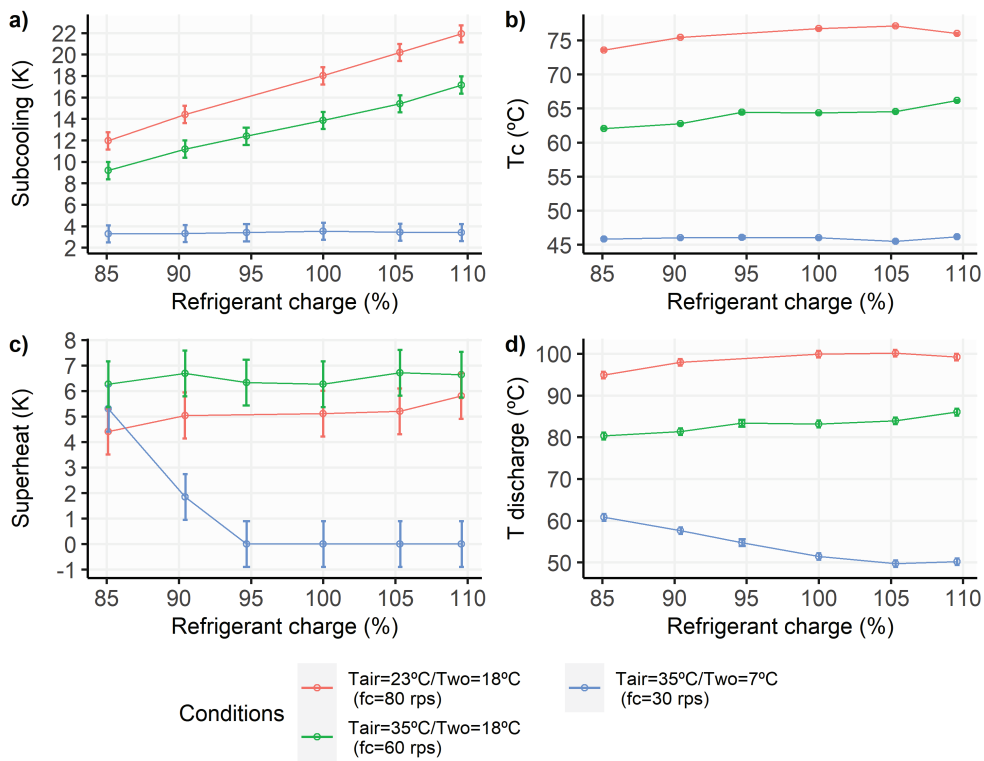


Fig. 4. Experimental measurements in cooling mode of a) subcooling, b) condensation temperature, c) superheat, and d) compressor discharge temperature.

3.2. Heating mode

In this mode, the EEV controls the SC at the condenser output instead of the SH. In this case, the SC target will be determined by a value that maximizes the COP in each condition, like the SH in cooling mode. Concerning the SH, the refrigerant in the liquid state will accumulate in the receiver at the evaporator outlet, ensuring saturation conditions and, therefore, SH of 0K. Table 4 shows the inputs to the model from the

measurements of each condition with 100% refrigerant charge. Thus, this table shows that the SH of each condition is 0K, being the evaporator outlet saturated and the target SC to be controlled by the EEV between 6 and 8 K, depending on the case. In addition, it is calculated with the model the refrigerant charge needed for each condition. Two conditions need more charge, A2W35-35rps, and A12W24-40rps, with required refrigerant charges of 0.53 and 0.47 kg, respectively. The A7W70-80rps and A10W45-80rps conditions need less refrigerant charge, both of them 0.35 kg.

Table 4. Refrigerant charge needed for each test condition in heating mode.

Test condition	Water inlet temperature (°C)	Water outlet temperature (°C)	Evaporator inlet temperature (°C) and Relative Humidity (%)	Airflow (m3/h)	Compressor Speed (rps)	SC (K)	SH (K)	Refrigerant charge (kg)
A2W35-35rps	32	35	2 (60.94%)	1229	35	6.7	0	0.526
A7W70-80rps	64	70	7 (53.51%)	1246	80	7.4	0	0.353
A10W45-80rps	38	45	10 (32.00%)	943	80	8	0	0.346
A12W24-40rps	20	24	12 (36.77%)	796	40	6.4	0	0.465

To analyze how the system performance develops with the refrigerant charge, it is studied the evolution with the charge of some variables from the condition that needs more charge, which is A2W35-35rps with 0.53 kg, and one that needs less, which is A7W70-80rps. Thus, in the case of A2W35-35rps and following Figure 5, as this condition requires more refrigerant charge to operate, it accumulates less liquid refrigerant charge in the receiver at the evaporator outlet. When a situation of undercharge or refrigerant leakage occurs, it will be reduced from the accumulator, as the liquid refrigerant at the outlet of the condenser (in this mode, the BPHX) will be fixed, and the EEV controls that the same amount is maintained to have the same SC value (Figure 7a). However, as this condition needs a lot of refrigerant charge to operate, it is already observed in Figure 7c that for a charge reduction of 5%, saturation conditions cannot be maintained at the outlet of the evaporator (i.e., the accumulator is with a low liquid level) and the SH increases to 2K. At 85% refrigerant charge, a SH of 12K is reached. Furthermore, for this test point, it is seen in Figure 7b how the evaporation pressure and, thus, the evaporating temperature decrease accordingly. Figure 7d shows the evolution of the discharge temperature with the refrigerant charge. It is observed that as the charge decreases, the discharge temperature increases by reducing the level of the accumulator, and the refrigerant enters the compressor with a lower vapor quality.

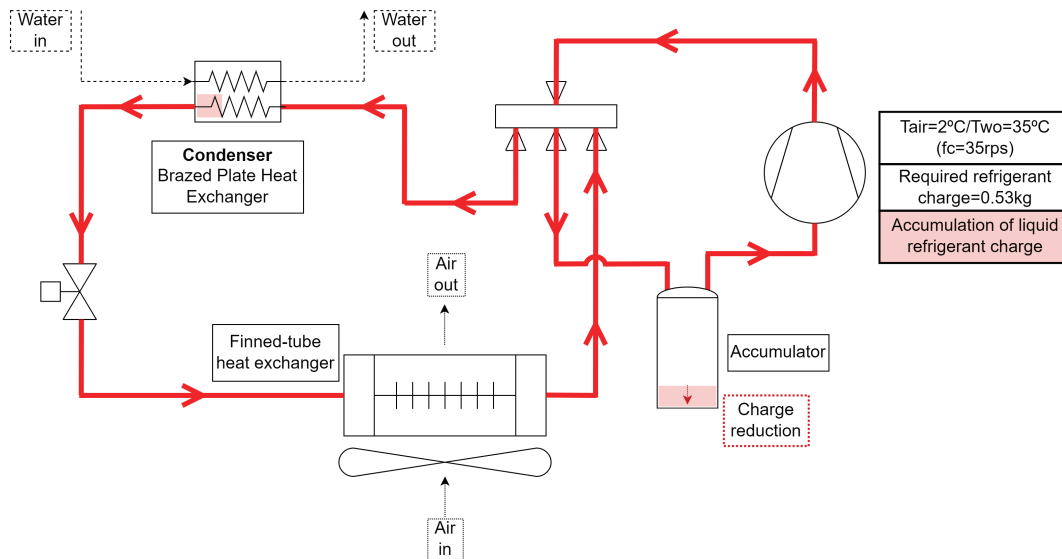


Fig. 5. Description of the accumulation of liquid refrigerant charge with the heating mode condition of $T_{air}=2^{\circ}C/T_{wo}=35^{\circ}C$ ($f_c=35rps$).

However, in the case of test condition A7W70-80rps, less refrigerant charge is needed than in the previously described condition. Therefore, it will accumulate more liquid refrigerant than in the previous case. This

refrigerant is collected in the accumulator at the evaporator outlet since, as in the previous case, the amount of refrigerant accumulated at the condenser outlet depends on the value controlled by the EEV, which will remain constant regardless of variations in the refrigerant charge (Figure 7a). Likewise, the refrigerant charge required to operate is lower, and the level of liquid refrigerant in the accumulator is higher, reducing the charge to 85% makes the level still enough to maintain saturation conditions at the outlet of the evaporator. Figure 7c shows how the SH is kept at 0K. Similarly, Figures 7b and 7d show how the evaporation and discharge temperature also do not vary when reducing the refrigerant charge, showing that the accumulator has a high refrigerant charge level.

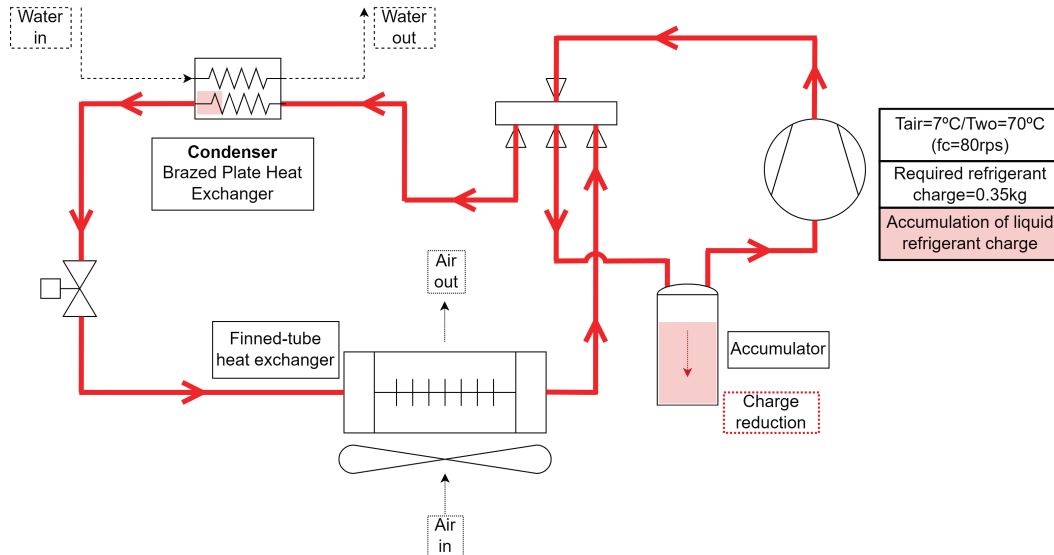


Fig. 6. Description of the accumulation of liquid refrigerant charge with the heating mode condition of $T_{air}=7^{\circ}\text{C}/T_{wo}=70^{\circ}\text{C}$ ($f_c=80\text{rps}$).

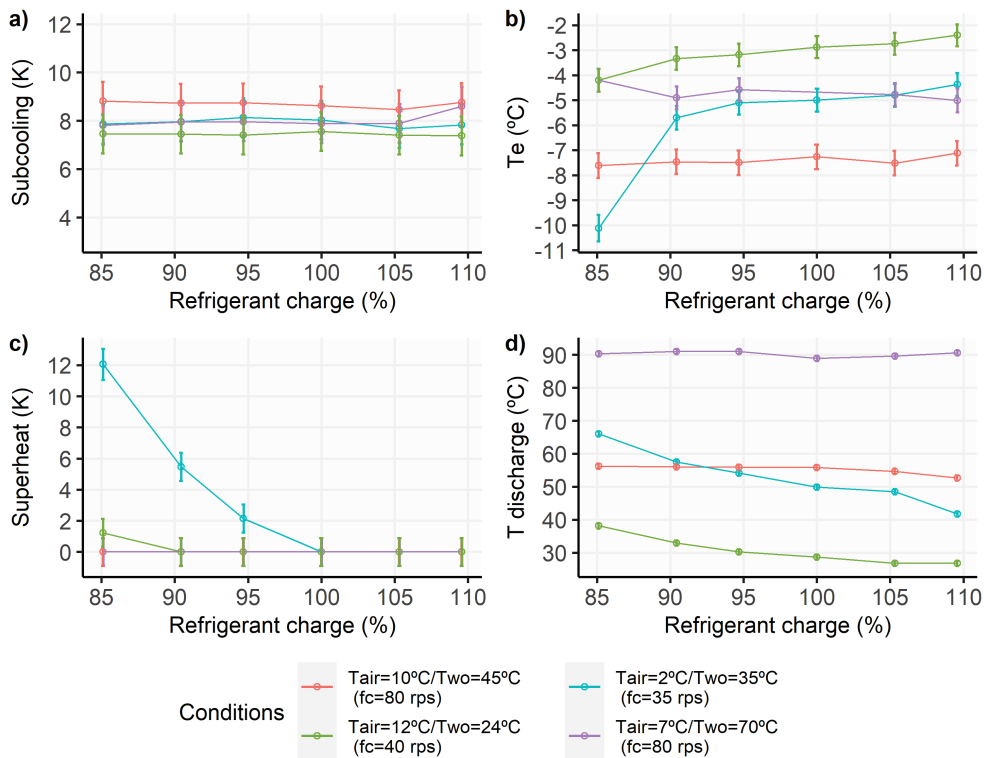


Fig. 7. Experimental measurements in heating mode of a) subcooling, b) evaporation temperature, c) superheat, and d) compressor discharge temperature.

With the experimental tests varying the refrigerant charge and the model it is possible to simulate the required charge in each condition, and it has been done a study varying some parameters. As it has been seen previously, the heat pump's performance will vary with the refrigerant charge depending on the condition. An analysis in heating mode has been done. Using the model, two usual application conditions in this mode have been selected ($T_{wi}=30^{\circ}\text{C}/T_{wo}=35^{\circ}\text{C}$ and $T_{wi}=65^{\circ}\text{C}/T_{wo}=70^{\circ}\text{C}$) changing the compressor speed and the air inlet conditions (evaporator inlet). The SC has been maintained constant with a value of 7 K and a SH=0K, since it is assumed that, there will be enough liquid refrigerant in the accumulator to have saturation conditions at the evaporator outlet.

The refrigerant charge required by the system for each case has been obtained. The results are shown in Figure 8. It is observed that for low compressor speeds and low air temperature, the system needs more charge to operate. This is mainly because of the variation in the compressor speed which changes the suction conditions. By decreasing the compressor speed, evaporating pressure and the density increase, requiring more refrigerant charge. The required charge will be slightly higher for the case of $T_{wi}=30^{\circ}\text{C}/T_{wo}=35^{\circ}\text{C}$ than for $T_{wi}=65^{\circ}\text{C}/T_{wo}=70^{\circ}\text{C}$. The zone denominated as "A" will have the performance previously described for A2W35-35rps (Figure 5). Since it needs more refrigerant charge to operate, the accumulator will have a lower liquid level. A 5% decrease in refrigerant charge will already cause changes in SH and discharge temperature, being much more pronounced with a 15% less charge. In the zone referred to as "B", the system needs a lower refrigerant charge to operate than in "A". It would be a refrigerant charge requirement similar to the tested conditions A12W24-40rps (0.47 kg). In this case, changes in discharge temperature and SH would be seen, but from a higher refrigerant reduction (15% in the case of the performed tests).

The rest of the contour plot that is not zone "A" or "B" in both T_{wi}/T_{wo} conditions will follow the performance described for the A7W70-70rps condition (Figure 6). In them, despite reducing the refrigerant charge by 15%, the charge requirements for that operating point can be satisfied because the accumulator still has a high liquid level. Considering this, if a refrigerant leak happens, no change in the operating variables could be observed for conditions outside of zones A and B.

Therefore, an undercharge fault diagnostic method to be explored in heating mode for this air-to-water heat pump with subcooling control can be to change the compressor speed to low values and, to a lower degree, reduce the water outlet temperature, bringing the system to zone A or B. With this, it can be seen if there are deviations from the typical values in the system variables that the heat pump would have in a given operating condition with a 100% refrigerant charge, such as the SH, the discharge temperature, or the evaporation temperature.

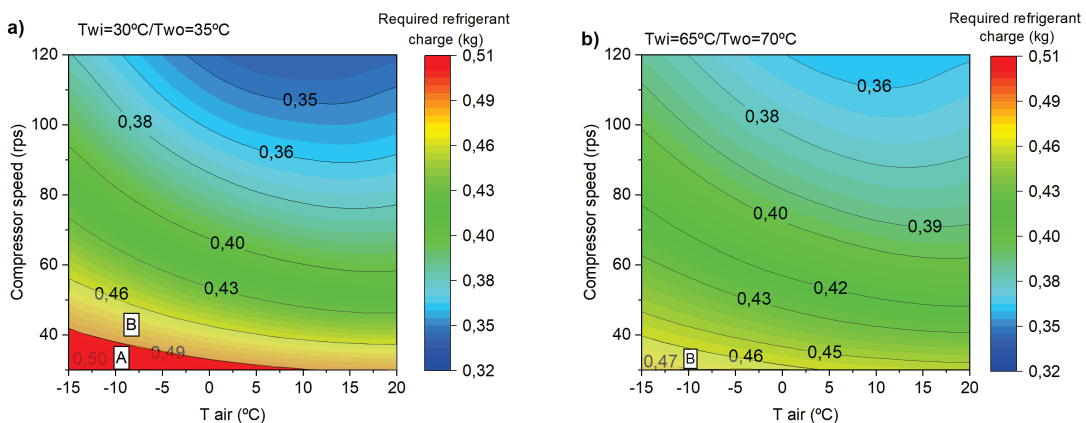


Fig. 8. Required system refrigerant charge with different compressor velocities and air inlet dry bulb temperature in heating mode. a) $T_{wi}=30^{\circ}\text{C}/T_{wo}=35^{\circ}\text{C}$, b) $T_{wi}=65^{\circ}\text{C}/T_{wo}=70^{\circ}\text{C}$.

4. Conclusions

This study presents an experimental campaign in which the dependence on the charge of a heat pump with a liquid receiver is analyzed, and it can be seen as a first step in order to determine future fault detection strategies in these systems. In cooling mode, the SH is controlled with an EEV, and in heating, the SC is controlled, having an accumulator that ensures SH=0K at the evaporator outlet. The study presents how the system variables change with the refrigerant charge and illustrates how the liquid refrigerant charge varies in the system in different conditions. Finally, the refrigerant charge required depending on the outdoor air conditions and compressor speed in heating mode is presented.

Some conclusions drawn are:

- In cooling mode, this system works by controlling the SH and therefore accumulating the refrigerant in a liquid state, mainly at the outlet of the condenser. Therefore, a refrigerant charge variation controlling SH>0K will cause the SC at the condenser outlet to increase or decrease as the charge increases or decreases respectively. The condensation temperature will also increase or decrease to a lower extent.
- In the case that the system controls the subcooling in cooling mode, a refrigerant charge higher than nominal will not cause changes. However, reducing it will cause changes in the discharge temperature and SH, as the liquid level in the accumulator will drop. The behaviour in these conditions is similar to the heating mode.
- In heating mode, the system controls the SC at the condenser outlet with the EEV, and the accumulator at the suction has a high refrigerant level, with SH=0. In conditions requiring a higher amount of charge, the accumulator will have a lower liquid level. Thus, reducing the refrigerant charge will increase the real SH and discharge temperature. Besides, to a lower degree, the evaporation temperature will drop.
- At these conditions, increasing the charge level will cause the discharge temperature to decrease and the evaporating temperature to increase slightly.
- At points that require a low refrigerant charge in heating mode, the accumulator level will be high, so by reducing the refrigerant charge by up to 15% in the tests, no changes in system variables are observed.
- In heating mode, at low compressor speeds, the heat pump needs more refrigerant charge to operate, being the more critical conditions from the charge point of view. The reduction of compressor speed in conditions that require a low refrigerant charge to diagnose an undercharge condition allows the observation of the deviation from the expected values in the discharge temperature and SH, so it results in an alternative to be explored in fault diagnosis of this kind of systems.

Nomenclature

BPHX	Brazed Plate Heat Exchanger	$m_{ref-nominal}$	Nominal refrigerant charge
EEV	Electronic Expansion Valve	A	Air inlet dry-bulb temperature
SH	Superheat	W	Water outlet temperature
SC	Subcooling	T_{wi}	Water inlet temperature
T	Temperature	T_{wo}	Water outlet temperature
P	Pressure	fc	Compressor speed
RH	Relative Humidity	Tc	Condensation temperature
$m_{ref-test}$	Refrigerant charge at a given test	Te	Evaporation temperature

Acknowledgements

The present work has been supported by the Spanish “Ministerio de Ciencia e Innovación”, through the project ref: PID2020-115665RB-I00 “Decarbonización de edificios e industrias con sistemas híbridos de bomba de calor”, and by the Spanish “Ministerio de Universidades” through the “Formación de Profesorado Universitario” program ref. FPU 19/04012.

References

- [1] European Parliament. *Directive 2010/31/EU of the European Parliament and of the Council of 19 May 2010 on the Energy Performance of Buildings.*; 2021. <http://data.europa.eu/eli/dir/2010/31/oj>
- [2] European Heat Pump Association (EHPA). *The European Heat Pump Market and Statistics Report 2022.*; 2022. <https://www.ehpa.org/market-data/market-report-2022/>
- [3] Du Z, Domanski PA, Payne WV. Effect of common faults on the performance of different types of vapor compression systems. *Appl Therm Eng.* 2016;98:61-72. doi:10.1016/j.applthermaleng.2015.11.108
- [4] Hu Y, Yuill DP, Ebrahimifakhar A, Rooholghodos A. An experimental study of the behavior of a high efficiency residential heat pump in cooling mode with common installation faults imposed. *Appl Therm Eng.* 2021;184 (July 2020):116116. doi:10.1016/j.applthermaleng.2020.116116
- [5] Kim W, Braun JE. Extension of a virtual refrigerant charge sensor. *Int J Refrig.* 2015;55:224-235. doi:10.1016/j.ijrefrig.2014.09.015
- [6] Behfar A, Yuill D. Numerical simulation of fault characteristics for refrigeration systems with liquid line receivers. *Int J Refrig.* 2020;119:11-23. doi:10.1016/j.ijrefrig.2020.05.003
- [7] Guzzardi C, Azzolin M, Lazzarato S, Del Col D. Refrigerant mass distribution in an invertible air-to-water heat pump: effect of the airflow velocity. *Int J Refrig.* 2022;138(October 2021):180-196. doi:10.1016/j.ijrefrig.2022.03.006
- [8] De Carvalho BYK, Hrnjak P. Evaluation Of Subcooling Control In Residential Heat Pumps Through Experimental And Model Analysis. In: *International Refrigeration and Air Conditioning Conference.* ; 2022.
- [9] Hervas-Blasco E, Pitarch M, Navarro-Peris E, Corberán JM. Study of different subcooling control strategies in order to enhance the performance of a heat pump. *Int J Refrig.* 2018;88:324-336. doi:10.1016/j.ijrefrig.2018.02.003
- [10] Corberán JM, González-Maciá J, Montes P, Blasco R. “ART”, a computer code to assist the design of refrigeration and air conditioning equipment. In: *International Refrigeration and Air Conditioning Conference.* ; 2002. <http://www.imst-art.com/>